EUROPEAN ORGANIZATION FOR NUCLEAR RESEARCH

Proposal to the ISOLDE and Neutron Time-of-Flight Committee

Evolution of single-particle states along $N = 127$: The $d(^{212}\mathrm{Rn},p)^{213}\mathrm{Rn}$ reaction.

January 6, 2021

D. K. Sharp[1], S. J. Freeman[1], S. A. Bennett[1], P. A. Butler[2], A Ceulemans[3], G. de Angelis[4], L. P. Gaffney[2], K. Garrett[1], C. R. Hoffman[5], B. P. Kay[5], M. Labiche[6], I. Lazarus[6], R. D. Page[2], O. Poleshchuk[3], R. Raabe[3], T. L. Tang[5] and the ISOLDE Solenoidal Spectrometer Collaboration

[1]*School of Physics and Astronomy, The University of Manchester, Manchester, M13 9PL, UK*
[2]*Oliver Lodge Laboratory, University of Liverpool, Liverpool, L69 7ZE, UK*
[3]*KU Leuven, Instituut voor Kern- en Stralingsfysica, 3001 Leuven, Belgium*
[4]*INFN, Laboratori Nazionali di Legnaro, 35020 Legnaro, Italy*
[5]*Physics Division, Argonne National Laboratory, Argonne, Illinois 60439, USA*
[6]*STFC Daresbury Laboratory, Daresbury, Warrington, WA4 4AD, UK*

Spokesperson: D. K. Sharp (david.sharp@manchester.ac.uk)
Co-spokesperson: S. J. Freeman (sean.freeman@manchester.ac.uk).
ISOLDE contact: Bruno Olaizola (bruno.olaizola@cern.ch)

CERN-INTC-2021-010 / INTC-P-594
06/01/2021

Abstract: We propose a measurement of the $^{212}\mathrm{Rn}(d,p)^{213}\mathrm{Rn}$ reaction in inverse kinematics, using the ISOLDE Solenoidal Spectrometer. The aim of the measurement is to characterise the neutron single-particle states along $N = 127$ - one neutron outside the $N = 126$ shell closure, north of $^{208}\mathrm{Pb}$. The neutron-adding reaction will probe spectroscopic overlaps for the $3s_{1/2}$, $2d_{5/2}$, $1g_{9/2}$, $0i_{11/2}$ and $0j_{15/2}$ neutron orbitals. These data will reveal the magnitude of the monopole shifts in these orbitals, arising from filling the $\pi 0h_{9/2}$ orbital. These data will also be compared to, and used to inform advances in, modern shell-model calculations to ascertain how well effective interactions are describing this evolution. We request 19 shifts of beam time for these measurements.

Requested shifts: 6 days + 1 shift (19 shifts), split into 1 run over 1 year.
Installation: ISOLDE Solenoidal Spectrometer

1 Physics case

Single-particle characteristics underlie many aspects of nuclear structure. The study of single-particle structure in light neutron-rich systems has led to discoveries of dramatic changes which are otherwise gradual near stability, leading to the weakening and appearance of shell closures. For example, the disappearance of $N = 20$ and emergence of $N = 16$ [1, 2] as well the emergence of $N = 32, 34$ in calcium isotopes [3]. Pronounced trends have also been observed in stable heavier nuclei, in the changes in high-j states as high-j orbitals are filling. Studies of chains of stable, closed-shell isotopes and isotones have pointed to fairly robust mechanisms for these changes, such as the importance of a tensor interaction [4]. To date we have studied the changes of the single-particle centroids for the single nucleon outside the $N = 50$ [5] and $N = 82$ [6] isotones and $Z = 50$ [7] isotopes, and the single-hole centroids below $N = 82$ [8] have been studied in a systematic fashion.

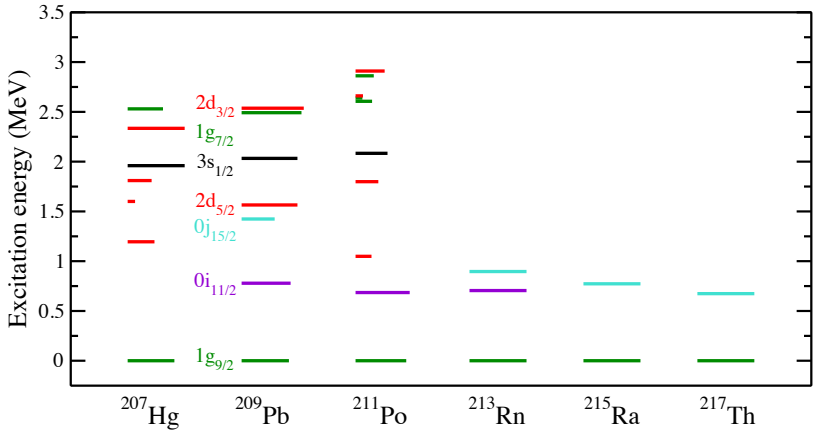

Figure 1: Known levels in $N = 127$ isotones. Width of bars indicate experimental spectroscopic factors, where known. Above $Z = 84$ there is no spectroscopic information on the states and only energies are known - along with tentative assignments.

The $N = 126$ isotones provide a region of the nuclear chart in to which to extend these studies, where the available stable systems to study are limited but the availability of the radioactive $N = 126$ beams at ISOLDE makes experiments possible. We have made the first studies of single-particle studies in a short-lived $N = 127$ nucleus, south of ^{208}Pb, via the measurement of the ^{206}Hg$(d,p)^{207}$Hg reaction [9]. However, data north of ^{208}Pb are also lacking, with the exception of a measurement of the ^{210}Po$(d,p)^{211}$Po reaction using a long-lived target [10]. In ^{213}Rn, and heavier $N = 127$ isotones, there are no firm spin assignments of states and the energies of only the first one or two excited states are known, a summary of known states for the $N = 127$ isotones is given in Fig. 1.

Along these isotones, as more protons are added, it is expected that the nodeless $\pi h_{9/2}$ orbital is filling. Any changes in the single-particle centroids for the single neutron outside $N = 126$, related to the effective single-particle energies, are likely to be attributed to the interaction with that neutron and the protons in this orbital, and especially pronounced for the nodeless neutron i and j states. In Figure 2 two-body matrix element calculations

are shown, shifted onto the known single-particle levels in ^{209}Pb, assuming filling of protons in the $h_{9/2}$ orbital. These calculations highlight the effect of the tensor interaction particularly in the monopole shifts of high-j orbitals. Identification of the single-particle states along the $N = 127$ isotones will reveal the evolution of single-particle strength outside $N = 126$ and test these monopole shift predictions. Further, with the $h_{9/2}$ dominantly filling up to $Z = 92$, it will be an important anchor point for predictions of neutron single-particle energies from Rn to U (near the proton drip-line).

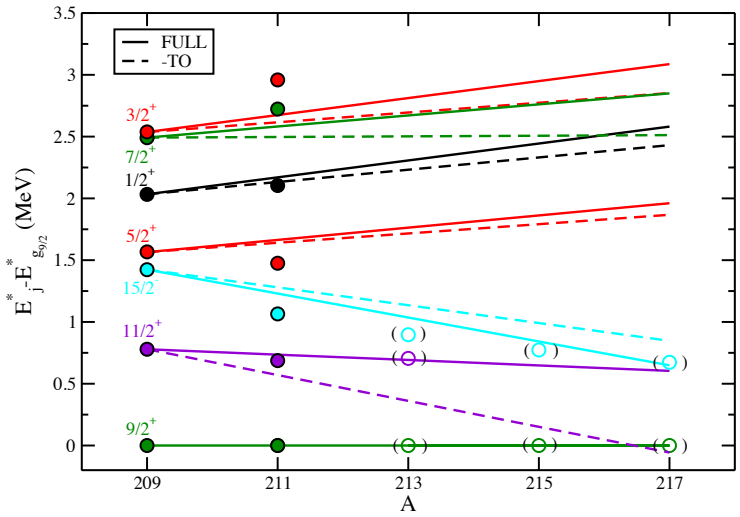

Figure 2: Two-body matrix element calculations of the neutron monopole shifts due to filling of the $h_{9/2}$ proton orbital, relative to the $g_{9/2}$ ground state. Calculations have been done with (FULL) and without (TO) the inclusion of a tensor operator using the two-body force from Ref. [11] and calculated using the computer code from Ref. [12]. The calculations are shifted onto the data at ^{209}Pb. The points are available experimental data, with parentheses denoting tentative assignments and hollow points where there are no available spectroscopic factors.

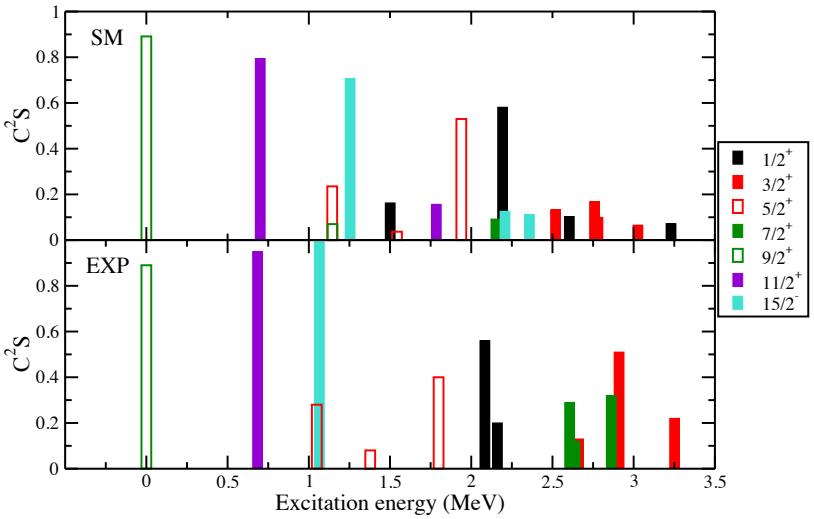

Figure 3: (Top) Spectroscopic factors from shell-model calculations for states populated via the (d,p) reaction in ^{211}Po, where $S > 0.05$ [13]. (Bottom) Experimental spectroscopic factors taken from Ref. [10].

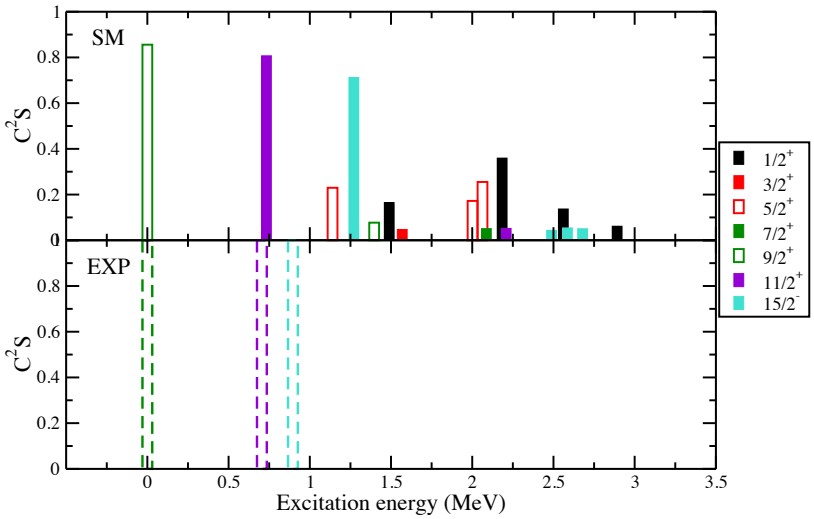

Figure 4: (Top) Spectroscopic factors from shell-model calculations for states populated via the (d,p) reaction in ^{213}Rn, where $S > 0.05$ [13]. (Bottom) Known experimental levels. Spectroscopic factors are not known and so are plotted here with a value of $C^2S = 1$.

The location of these nuclei, with one neutron outside the $N = 126$ shell closure and in the vicinity of doubly-magic ^{208}Pb, makes them ideal for testing modern shell-model calculations. Shell-model calculations, done using the Kuo-Herling interaction [14], are shown in Figures 3 and 4 for states in ^{211}Po and ^{213}Rn, respectively, along with the known experimental information, which is distinctly lacking for Rn. These shell-model calculations describe the strength distribution in ^{211}Po well, with perhaps the exception of the $d_{3/2}$ and $g_{7/2}$ strength, which is observed to be relatively stronger than predicted.

There are also hints at deviations from the calculations for ^{213}Rn, for example in the energy of the $j_{15/2}$, but again there is a lack of information in this region.

2 Experimental details

Transfer reactions are the ideal tool for studying single-particle properties of nuclei. Under the right experimental conditions they provide selective population of single-particle states. Comparison of measured transfer cross sections to reaction models allows the extraction of spectroscopic factors, a measure of the single-particle strength of a populated state. The centroid of single-particle strength, for a particular shell-model orbital, is related to the effective single-particle energy for that orbital. These are key ingredients for explaining the roles of different components of the nucleon-nucleon interaction in the evolution of single-particle structure.

Reaction and beam properties—We propose to measure single-neutron transfer in inverse kinematics to probe the single-particle structure in $N = 127$ isotones at an incident beam energy of 7.5 MeV/u. The highest available beam energy is required to maximise the cross section for population of the final states of interest, especially high-ℓ transfers. The dependence of the integrated cross section (defined by the detector acceptance) on beam energy is given in Figure 5, highlighting the gains made with even incremental increases in beam energy. The angular distributions also become more pronounced at forward centre-of-mass angles with increasing beam energy, making identification of the transferred angular momentum easier, shown for example in Fig. 6. Beams of $>$ 95% purity are required for these measurements, as recoil detection will not assist in identification here. The ^{212}Rn beam is expected to be clean through the use of a cooled transfer line, as delivered to Miniball in IS506 [15].

ISOLDE Solenoidal Spectrometer—In inverse kinematics, a heavy beam is incident on a light target, in this case deuterated polyethylene (CD_2). The protons from the (d,p) reaction, at the forward centre-of-mass angles of interest, are emitted at backwards laboratory angles, relative to the incident beam direction. We intend to use the ISS in order to momentum analyse the outgoing protons, measuring their energies and yields to final states in ^{213}Rn. Measurements have previously been made using the ISS in this mass region for the ^{206}Hg(d,p) reaction [9], where a Q-value resolution of 140 keV FWHM was achieved, using the position-sensitive array from the HELIOS spectrometer [16], and targets with a nominal thickness of 165 μg/cm^2. For the current measurement, the new silicon array and associated electronics developed by the UK ISS collaboration will be used. A Q-value resolution of $<$140 keV should be achievable with this new instrumentation, as well as the use of thinner targets. The extracted cross sections and angular distributions will be compared to calculations using the finite-range DWBA code Ptolemy [17] to obtain information on the ℓ value of the final states and spectroscopic factors.

Given the level density and spacing given by the shell-model calculations in Fig. 4, one should expect to extract proton yields for most of the final states of interest without much difficulty. There will be potential doublets but there are methods to mitigate

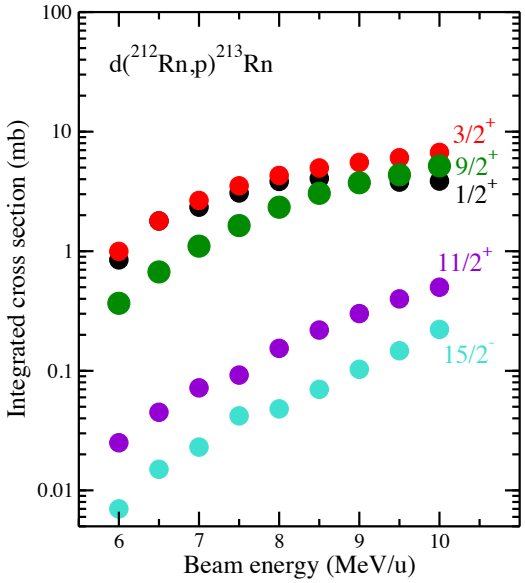

Figure 5: Integrated cross sections calculated using DWBA for final states populated in the ^{212}Rn$(d,p)^{214}$Rn reaction, assuming $S = 1$, as a function of the incident beam energy.

these, such as fitting combined yields with sums of calculated angular distributions, to extract the angular momentum transfer. As with the measurement with ^{206}Hg, a smoothly varying background of charged-particles, from fusion-evaporation of the beam with the target, will be present but this should not overly complicate the extraction of yields. Applying a timing condition in relation to the EBIS release will help to remove some of the background.

3 Proposed experiment

Experimental set-up—For the measurements proposed here, the silicon array will be positioned −9.9 cm from the target as measured to the nearest detector edge, covering a range in z from the target of −9.9 to −60.0 cm. The solenoid field will be set at 2.0 T. With these settings, protons emitted at $10° < \theta_{cm} < 40°$ will be incident on the array for all states up to 3 MeV. Elastically-scattered deuterons will be detected in a silicon monitor detector positioned at $z = +15$ cm, corresponding to $\theta_{cm} = 20°$. A bespoke Faraday cup, that will be suppressed despite the magnetic field of ISS, will be positioned in front of the monitor detector to measure the delivered beam dose. This Faraday cup/monitor detector arrangement will be mounted on a moveable arm along with an ISOLDE Faraday cup - for tuning purposes. Given the expected degradation of CD_2 targets with beams of this mass then a target ladder adapted to hold 64 targets will be used, in order to reduce the need for opening of ISS to change targets.

Beam time request—A beam intensity of 1×10^6 pps of ^{212}Rn has been assumed, based on the values given in the yield database, an assumption of an average proton current of $1.5\mu A$ and a total transmission efficiency to ISS of 3% [18]. At these rates, there will

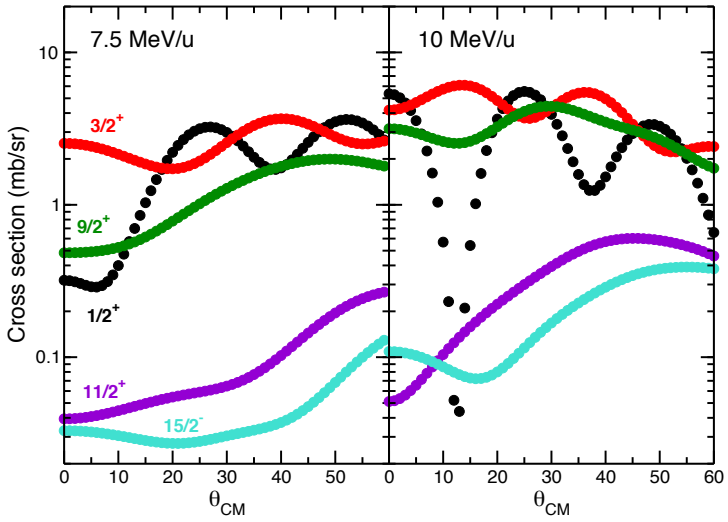

Figure 6: Angular distributions calculated using DWBA for final states populated in the ^{212}Rn(d,p)^{214}Rn reaction, assuming $S = 1$, for beam energies of 7.5 MeV/u and 10 MeV/u

be ∼600, 750, 350, 20 and 10 counts per day in the whole array for $s_{1/2}$, $d_{5/2}$, $g_{9/2}$, $i_{11/2}$ and $j_{15/2}$ states, respectively, assuming $S = 1$. The array has an efficiency of 70% in the azimuthal angle and 94% in the theta angle. The CD_2 targets will be ∼100 μg/cm^2 thick. Cross sections were estimated using the finite-range DWBA code Ptolemy and optical-model parameters of An and Cai [19] and Koning and Delaroche [20] for the deuteron and proton, respectively. The target and projectile bound-state parameters given in Ref. [21] were used.

The aim here is to study, for the first time, the location of excited states in these $N = 127$ isotones, the single-particle content and distribution of single-particle strength for low-j states. The changes in the centroid of single-particle strength will point to the magnitude of monopole-shifts along $N = 127$, with changing proton occupancy. A secondary goal is the confirmation of the location of any of the high-j states. **18 shifts** of ^{212}Rn beam on target would be required to achieve yields of ∼100 counts in the $i_{11/2}$ level ($S = 0.8$), in order to identify the likely candidate for this state above background. This level of statistics will also allow a robust study of the more fragmented low-j states with $700 - 1000$ total counts in each of the largest fragments of these, with $S > 0.2$. We also request a further **1 shift** in order to optimise the radioactive beam into the spectrometer. It should be noted that an obvious extension to this study, yields permitting, would be the ^{214}Ra(d,p)^{215}Ra reaction. We are in contact with the ISOLDE target team to better understand the yields of ^{214}Ra and would submit a follow-up proposal were this measurement to be confirmed as feasible.

Summary of requested protons: 19 shifts of protons are requested for this measurement.

References

[1] A. Ozawa *et al.,* Phys. Rev. Lett. **84**, 5493 (2000).
[2] C. R. Hoffman *et al.,* Phys. Lett. B **672**, 17 (2009).
[3] D. Steppenbeck *et al.,* Nature **502**, 207 (2013).
[4] T. Otsuka *et al.,* Phys. Rev. Lett. **95**, 232502 (2005).
[5] D. K. Sharp *et al.,* Phys. Rev. C **87**, 014312 (2013).
[6] B. P. Kay *et al.,* Phys. Lett. B **658**, 216 (2008).
[7] J. P. Schiffer *et al.,* Phys. Rev. Lett. **92**, 162501 (2004).
[8] A. M. Howard *et al.,* Phys. Rev. C **101**, 034309 (2020).
[9] T. L. Tang *et al.,* Phys. Rev. Lett. **124**, 062502 (2020).
[10] T. S. Bhatia *et al.,* Nuc. Phys. A. **314**, 101 (1979).
[11] A. Hosaka, K. I. Kubo and H. Toki, Nuc. Phys. A. **444**, 76 (1985).
[12] A. Etchegoyen, M. C. Etchegoyen, and E. G. Vergini, Comput. Phys. Commun. 55, 227 (1989).
[13] B. A. Brown, (Private communication).
[14] E. K. Warburton and B. A. Brown Phys. Rev. C **43**, 602 (1991).
[15] T. Grahn, IS506
[16] A. H. Wuosmaa *et al.,* Nucl. Instrum. Meth. A, **580**, 1290 (2007).
[17] M. H. Macfarlane and S. C. Pieper, ANL-76-11 Rev. 1, ANL Report (1978).
[18] J. A. R. Rodriguez, (Private communication).
[19] H. An and C. Cai, Phys. Rev. C **73**, 054605 (2006).
[20] A. J. Koning and J. P. Delaroche, Nuc. Phys. A. **713**, 231 (2003).
[21] B.P. Kay, J.P. Schiffer and S.J. Freeman, Phys. Rev. Lett. **111** 042502 (2013).

Appendix 1

DESCRIPTION OF THE PROPOSED EXPERIMENT

The experimental setup comprises: The ISOLDE Solenoidal Spectrometer

Part of the	Availability	Design and manufacturing
ISOLDE Solenoidal Spectrometer	☒ Existing	☒ To be used without any modification ☐ To be modified
	☐ New	☐ Standard equipment supplied by a manufacturer ☐ CERN/collaboration responsible for the design and/or manufacturing

HAZARDS GENERATED BY THE EXPERIMENT (if using fixed installation:) Hazards named in the document relevant for the fixed ISS installation.

Additional hazards:

Hazards			
Thermodynamic and fluidic			
Pressure			
Vacuum			
Temperature			
Heat transfer			
Thermal properties of materials			
Cryogenic fluid			
Electrical and electromagnetic			
Electricity			
Static electricity			
Magnetic field	2.0 T		
Batteries			
Capacitors			
Ionizing radiation			
Target material	Deuterated polyethylene (50-400 μg/cm^2)		
Beam particle type	^{212}Rn		
Beam intensity	1×10^6		
Beam energy	7.5 MeV/u		
Cooling liquids			
Gases			
Calibration sources:	☒		
• Open source	☒ (α calibrations source 4236RP)		
• Sealed source			

• Isotope	^{148}Gd, ^{239}Pu, ^{241}Am, ^{244}Cm		
• Activity	1 kBq, 1 kBq, 1 kBq, 1 kBq = 4 kBq		
Use of activated material:			
• Description			
• Dose rate on contact and in 10 cm distance			
• Isotope			
• Activity			
Non-ionizing radiation			
Laser			
UV light			
Microwaves (300MHz-30 GHz)			
Radiofrequency (1-300 MHz)			
Chemical			
Toxic			
Harmful			
CMR (carcinogens, mutagens and substances toxic to reproduction)			
Corrosive			
Irritant			
Flammable			
Oxidizing			
Explosiveness			
Asphyxiant			
Dangerous for the environment			
Mechanical			
Physical impact or mechanical energy (moving parts)			
Mechanical properties (Sharp, rough, slippery)			
Vibration			
Vehicles and Means of Transport			
Noise			
Frequency			
Intensity			

Physical			
Confined spaces			
High workplaces			
Access to high workplaces			
Obstructions in passageways			
Manual handling			
Poor ergonomics			

Hazard identification:

Average electrical power requirements (excluding fixed ISOLDE-installation mentioned above): N/A